ChemPlusChem

Research Article
doi.org/10.1002/cplu.202400031

Chemistry Europe
European Chemical Societies Publishing

www.chempluschem.org

1- and 2-Tetrazolylacetonitrile as Versatile Ligands for Laser Ignitable Energetic Coordination Compounds

Simon M. J. Endraß,[a, b] Thomas M. Klapötke,[a, b] Marcus Lommel,[a, b] Jörg Stierstorfer,*[a, b] Martin L. Weidemann,[a] and Melanie Werner[a]

On the occasion of Prof. Dr. Ingo-Peter Lorenz 80th Birthday

1- and 2-Tetrazolylacetonitrile (1- and 2-TAN) have been synthesized by the reaction of chloroacetonitrile with 1*H*-tetrazole under basic conditions. They further were reacted with sodium azide in the presence of zinc(II) chloride to form 5-((1*H*-tetrazol-1-yl)methyl)-1*H*-tetrazole (1-HTMT) and 5-((2*H*-tetrazol-2-yl)methyl)-1*H*-tetrazole (2-HTMT). The nitrogen-rich compounds have been applied as ligands for Energetic Coordination Compounds (ECCs) and show interesting coordinative behavior due to different bridging modes. The structural variability of the compounds has been proved by low-temperature X-ray analysis. The ECCs were analyzed for their sensitivities to provide information about the safety of handling and their capability to serve as primary explosives in detonator setups to replace the commonly used lead styphnate and azide. All colored ECCs were evaluated for their ignitability by laser initiation in translucent polycarbonate primer caps. In addition, the spin-crossover characteristics of $[Fe(1\text{-}TAN)_6](ClO_4)_2$ were highlighted by the measurement of the temperature-dependent susceptibility curve.

Introduction

Nitrile groups are versatile functionalities, which are of great interest for synthetic chemists. They allow the preparation of amines and aldehydes by reduction,[1] the formation of amides or carboxylic acids,[2] ketones and tertiary amines by reaction with metal-organic Grignard reagents,[3] as well as tetrazole moieties by 1,3-dipolar cycloadditions.[4] In addition, the nitrile function allows the formation of coordination compounds with a broad range of transition metals.[5] By combining this easily available side chain functionality with the coordinative behavior and high enthalpy of formation of the tetrazole ring, 2-(1*H*-tetrazol-1-yl)acetonitrile and 2-(2*H*-tetrazol-2-yl)acetonitrile (1- and 2-TAN) can be formed and used for complexation of transition metals.[6] This enables the formation of high-nitrogen Energetic Coordination Compounds (ECCs) with high positive heats of formation. Due to their slightly different donor sites, they might be characterized as *Janus Head* ligands.[7] This allows the adjustability of the composition of the ECC, due to the increase of coordination of the less favored site upon the reduction of equivalents used. While in other cases the goal of the *Janus Head* ligand is to combine functional groups that allow coordination to different cations on the two sites and hereby achieve e.g. catalytic activity, the idea of the TAN ligands was to improve and study the ligand to anion ratio in the ECCs.[8] By adding the possibility to coordinate to the tetrazole ring as well as the nitrile function, different stoichiometric relations of ligand and oxidizer in the ECCs, and therefore beneficial properties, might be obtained.[9] Figure 1 shows examples of CHN-based tetrazole ligands, which have been previously applied in ECCs. For these cases, only ligand-to-perchlorate ratios of 3:1 were obtained by complexation of Cu(II)-, Fe(II)- and Zn(II)-perchlorate.

This work seeks to introduce 1- and 2-TAN as building blocks for ECCs with the possibility to alter the coordination mode and observe the desired impact on the energetic properties. In addition, previous publications have shown the possibility of creating acidic *C*-linked tetrazoles, which are derived from nitrile functionalities and can be used for the formation of energetic salts.[6a,11] Therefore, ring-closure of respectively 1- and 2-TAN was performed to obtain 5-((1*H*-tetrazol-1-yl)methyl)-1*H*-tetrazole (1-HTMT) and 5-((2*H*-tetrazol-2-yl)methyl)-1*H*-tetrazole (2-HTMT). Those two molecules possess high nitrogen contents of above 70%. Furthermore, they allow for different bridging modes between metal centers and the ratio of ligand to additional anion compared to the *N,N*-ditetrazolylmethane ligands, which have successfully been applied in primary explosives and for laser initiation.[12]

[a] S. M. J. Endraß, Prof. Dr. T. M. Klapötke, M. Lommel, Dr. J. Stierstorfer, M. L. Weidemann, M. Werner
Department of Chemistry
Ludwig-Maximilians-Universität München
Butenandtstr. 5–13, 81377 Munich, Germany
E-mail: jstch@cup.uni-muenchen.de

[b] S. M. J. Endraß, Prof. Dr. T. M. Klapötke, M. Lommel, Dr. J. Stierstorfer
EMTO GmbH,
Energetic Materials Technology
81477 Munich, Germany

Supporting information for this article is available on the WWW under https://doi.org/10.1002/cplu.202400031

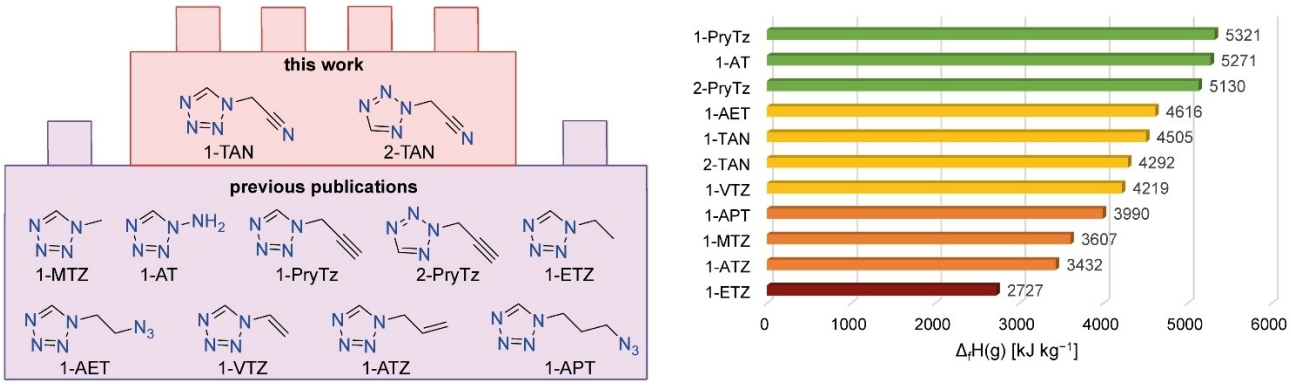

Figure 1. Examples of previously published mono-tetrazole ligands as building blocks for energetic coordination compounds which are based on CHN including their gas-phase enthalpies of formation.[10]

Results and Discussion

Synthesis

The two ligands of interest (1- and 2-TAN) were obtained by a chloride-tetrazolate exchange reaction. As seen in Scheme 1, the reaction was performed in a mixture of acetonitrile and acetone (5:1) to exploit the solvent dependent stabilization, and therefore obtain equal amounts of both isomers.[13] After the reaction, purification was conducted by column chromatography in EtOAc/iHex (1:1) to obtain a moderate overall yield of 68%. Both compounds were obtained as yellow liquids, however samples of **1** crystallized after several weeks of storage at 4 °C. Therefore, the crystal structure and melting point could be obtained.

One important goal of the research on ECCs is their potential to serve as replacements for lead azide and lead styphnate in detonators and primer caps. The main reason for this is the toxicity of lead.[14] The need for replacements was further manifested in the restrictions on the use of both substances, which were enacted by the European Union.[15] Promising candidates as successors of lead azide and lead styphnate, that are known to literature, are ECCs based on copper(II) azide.[16] Attempts to prepare copper(II) azide complexes with **1** and **2** lead to impure products according to elemental analysis. Therefore, layering experiments were conducted to investigate the possible species. A solution of sodium azide and ligand in water was separated from an ethanolic solution of copper(II) chloride by a 1:1 mixture of ethanol and water. The slow mixing of the layers leads to the formation of a single crystal in the case of the 1-TAN ligand. Single crystal analysis revealed the formation of 5-((1*H*-tetrazol-1-yl)methyl)tetrazol-1-ide as one of the products, most likely in a copper-catalyzed manner. To investigate the behavior of this anion further, the neutral compounds were prepared by zinc-catalyzed click chemistry as proposed by *Demko* and *Sharpless* (Scheme 2).[17] The obtained 5-((1*H*-tetrazol-1-yl)methyl)-1*H*-tetrazole (1-HTMT) and 5-((2*H*-tetrazol-2-yl)methyl)-1*H*-tetrazole (2-HTMT) were analyzed concerning their energetic properties and applicability of their anions for the formation of ECCs.

1- and 2-TAN were applied in coordination compounds of different transition metal perchlorates and copper(II) nitrate. Transition metals which are known for their high toxicity levels like chromium, cobalt and nickel were excluded.[18] An overview of successful complexation attempts is given in Scheme 3. Attempts of complexation with $Mn(ClO_4)_2 \cdot 6\,H_2O$ were discarded due to the formation of MnO_2 within one day. Complexation of most perchlorates with **2** did not lead to a solid product and were therefore of no interest for this work.

Scheme 4 shows the ECCs of 1-TAN with copper salts of nitroaromatic anions. To obtain those, the respective nitrophenol (H_3TNPG: trinitrophloroglucinol, H_2TNR: styphnic acid, HPA: picric acid, H_2TNO: trinitro–orcinol) was combined with basic copper carbonate and water and heated to 80 °C until a clear solution was obtained. To these solutions, the ligand was

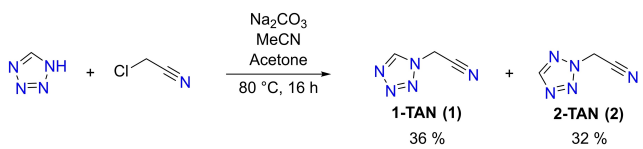

Scheme 1. Synthesis of 1- and 2-tetrazolylacetonitrile.

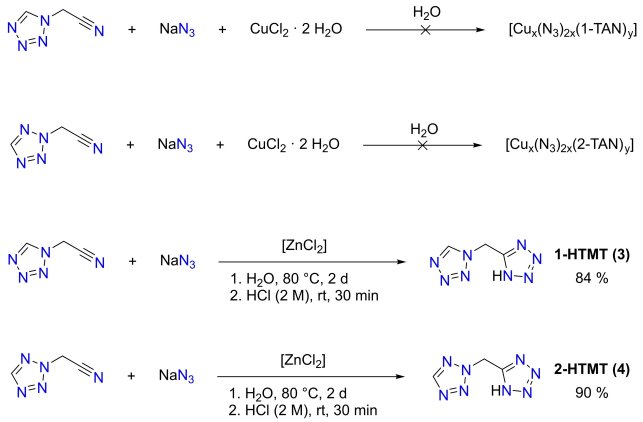

Scheme 2. Formation of 1- and 2-HTMT by zinc-catalyzed tetrazole-ring closure to the nitrile groups of 1- and 2-TAN.

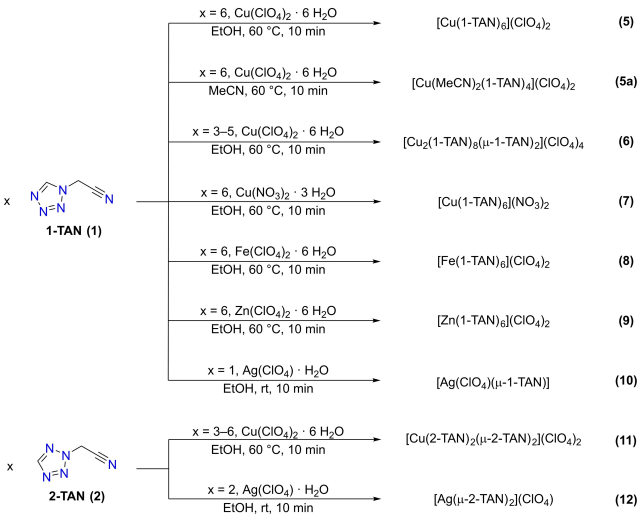

Scheme 3. Complexation of transition metal perchlorates and nitrates with 1- and 2-TAN.

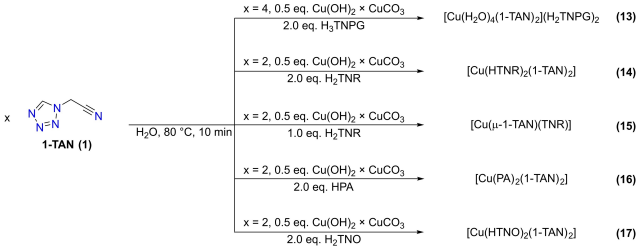

Scheme 4. ECCs with nitroaromatic anions that contain the 1-TAN ligand.

added under stirring. After stirring for 10 minutes at 80 °C, the solution was allowed to cool to room temperature. Since the usual coordination pattern of the copper(II) trinitrophloroglucinate complexes involves four ligands and coordination by the nitroaromatics hydroxides, there might be possible side species along the structure that was observed by single crystal X-ray diffraction. Unlike expected, 1-TAN functions as a bridging ligand in **16**, allowing for a ratio of copper, anion, and ligand of 1 : 1 : 1.

As seen in Scheme 5, the copper(II) trinitrophloroglucinate complex that was produced from 2-TAN showed some irregularities as well. The nitrile functionality of the ligand was hydrolyzed, and 2-(2*H*-tetrazol-2-yl)acetamide (2-TAA) was incorporated instead, which lead to impurity according to elemental analysis.

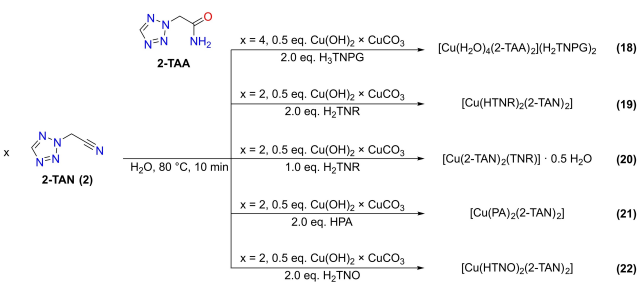

Scheme 5. ECCs derived from the 2-TAN ligand with nitroaromatic anions.

Scheme 6 shows that copper(II) azides with both, azide and tetrazolate anion were formed by deprotonation of **3** or **4** in the presence of sodium azide, followed by subsequent addition of copper(II) sulfate pentahydrate in aqueous solution. Species **23** was also obtained from 1-TAN by attempting the formation of $[Cu_x(N_3)_{2x}(1\text{-TAN})_y]$, as mentioned in Scheme 2. Copper(II) azides with additional negative anions that have recently been published, proved their thermal stability and were tested as sensitive in levels which appear to be interesting tradeoffs between performance and handling.[19]

Crystal Structures

All compounds, except for **2**, which was only obtained as a liquid, **15**, **21** (low crystal quality) and **24**, which precipitated as an amorphous solid, were analyzed by low-temperature X-ray diffraction analysis.[20] Structures were solved using the Olex2 software suite[21] using SHELXT[22] and refined using the full-matrix least squares method on *F2* by SHELXL.[23] Graphical illustration of the solved structures was performed using DIAMOND4,[24] showing non-hydrogen atoms as thermal ellipsoids at 50% probability level and hydrogen atoms as small spheres of arbitrary radius. Crystal structures, that are not shown in this section can be found in the Supporting Information. Figure 2 shows the crystal structures of the nitrogen-rich ligands a) 1-TAN, b) 1-HTMT, and c) 2-HTMT. While **1** ($P2_12_12_1$) and **3** (*Pbca*) crystallized in orthorhombic space groups, **4** was obtained in the monoclinic space group *Cc*. Recalculation of the X-ray densities to room temperature results in densities of 1.50 g cm^{-3} for 1-TAN and close to 1.60 g cm^{-3} for both 1-HTMT and 2-HTMT. These densities were used for the calculation of the detonation parameters by EXPLO5.[25] The copper(II), iron(II) and zinc(II) coordination compounds showed coordination patterns in form of distorted octahedrons. In the cases of $[Fe(1\text{-TAN})_6](ClO_4)_2$ and $[Zn(1\text{-TAN})_6](ClO_4)_2$ the deviation from a perfect octahedron can be found in the angles between the coordination bonds, which slightly differ from 90°, while all coordination bonds show similar length due to the high symmetry of the trigonal *R*−3 space group in which both crystallized. Figure 3 shows the difference in the structure of $[Fe(1\text{-TAN})_6](ClO_4)_2$ a) below and b) above the temperature at which the spin-crossover (SCO) was observed. Since both

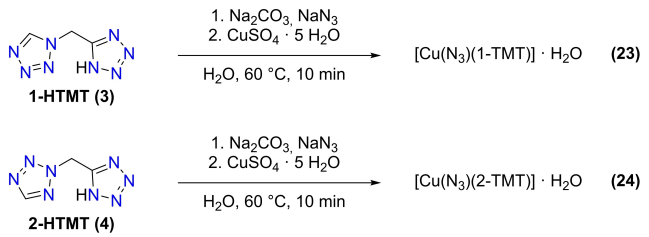

Scheme 6. Copper(II) azides **23** and **24**, with the tetrazolate anions 1-TMT and 2-TMT.

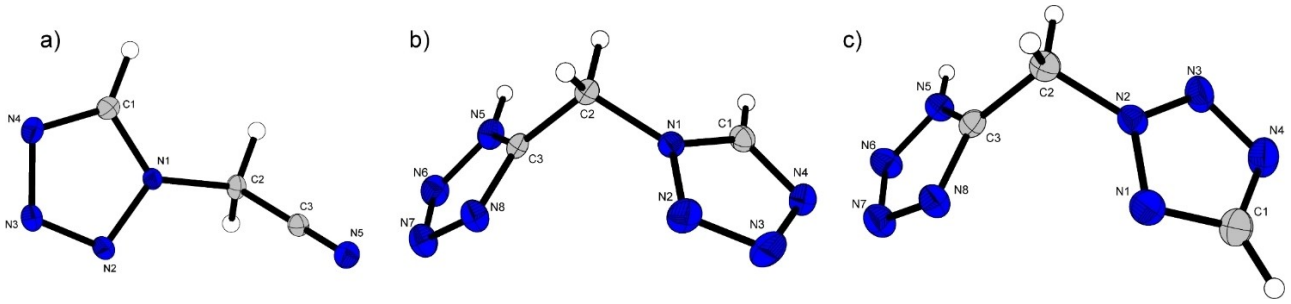

Figure 2. Crystal structures of a) 1-TAN, Selected bond lengths [Å]: N1–N2 1.3477(16), N5–C3 1.1398(16), N1–C1 1.3356(18), C2–C3 1.4710(16), N1–C2 1.4559(16), N2–N3 1.2972(17), N3–N4 1.3654(16), N4–C1 1.3136(19); Selected bond angles [°]: N2–N1–C1 108.71(11), N5–C3–C2 179.03(14), N2–N1–C2 121.85(10), C1–N1–C2 129.26(11), N1–N2–N3 105.90(10), N2–N3–N4 111.02(11), N3–N4–C1 105.42(12), N1–C1–N4 108.96(13), N1–C2–C3 110.80(10); b) 1-HTMT, Selected bond lengths [Å]: N1–N2 1.3405(17), N1–C1 1.3353(18), N1–C2 1.4713(17), N5–N6 1.3413(19), N5–C3 1.3378(17), N8–N7 1.3531(18), N8–C3 1.3229(18), N2–N3 1.303(2), N6–N7 1.306(2), N4–N3 1.345(2), N4–C1 1.3235(19), C3–C2 1.4850(19); Selected bond angles [°]: N2–N1–C2 121.86(12), C1–N1–N2 108.52(12), C1–N1–C2 129.61(13), C3–N5–N6 108.70(13), C3–N8–N7 105.64(12), N3–N2–N1 106.09(12), N7–N6–N5 106.10(12), N6–N7–N8 110.93(12), C1–N4–N3 105.60(13), N5–C3–C2 126.69(13), N8–C3–N5 108.63(12), N8–C3–C2 124.68(12), N2–N3–N4 111.13(12), N4–C1–N1 108.65(14), N1–C2–C3 110.81(11); c) 2-HTMT, Selected bond lengths [Å]: N5–N6 1.342(3), N5–C3 1.328(3), N2–N3 1.312(3), N2–N1 1.330(3), N2–C2 1.456(3), N8–N7 1.359(3), N8–C3 1.318(3), N6–N7 1.298(3), N3–N4 1.321(3), N1–C1 1.325(3), N4–C1 1.341(3), C3–C2 1.494(3); Selected bond angles [°]: C3–N5–N6 109.04(19), N3–N2–N1 114.40(19), N3–N2–C2 122.50(19), N1–N2–C2 123.08(18), C3–N8–N7 105.96(18), N7–N6–N5 106.19(18), N6–N7–N8 110.41(18), N2–N3–N4 105.92(19), C1–N1–N2 100.77(18), N3–N4–C1 105.79(19), N5–C3–C2 126.92(19), N8–C3–N5 108.39(18), N8–C3–C2 124.67(19), N2–C2–C3 110.77(17), N1–C1–N4 113.1(2).

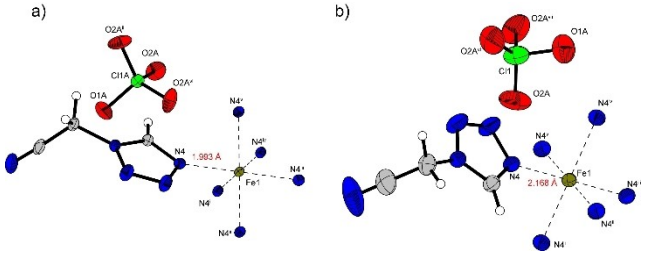

Figure 3. Crystal structures of $[Fe(1\text{-}TAN)_6](ClO_4)_2$ at a) 93 K; Selected bond lengths [Å]: Fe1–N4 1.9925(17); Symmetry codes: (i): −y, x−y, z; (ii): −x+y, −x, z; (iii): −x, −y, 1−z; (iv): y, −x+y, 1−z; (v): x−y, x, 1−z; (vi): 1−y, x−y, z; (vii): 1−x+y, 1−x, z; and b) 193 K; Selected bond lengths [Å]: Fe1–N4 2.1680(16); Symmetry codes: (i): 2−x, 1+x−y, z; (ii): 1+x−y, x, 1−z; (iii): 2−x, 2−y, 1−z; (iv): y, 1−x+y, 1−z; (v): 1−x+y, 2−x, z; (vi): −x+y, 1−x, z; (vii): 1−y, 1+x−y, z.

structures were obtained by measurement of the same single crystal, the structural changes, such as the shortened coordination bond, can be seen as a result of the SCO.

The structural variety increases in the case of the three differently coordinated copper(II) perchlorates $[Cu(1\text{-}TAN)_6](ClO_4)_2$ (**5**), $[Cu_2(1\text{-}TAN)_8(\mu\text{-}1\text{-}TAN)_2](ClO_4)_4$ (**6**) and $[Cu(2\text{-}TAN)_2(\mu\text{-}2\text{-}TAN)_2](ClO_4)_2$ (**11**). Crystallization of **5** occurs in the triclinic space group $P\bar{1}$ with three formula units per unit cell. The coordination sphere (Figure 4) shows the typical *Jahn-Teller* elongation distortion, that is expected for the d^9-case.

By reducing the amount of ligand that is used to five equivalents, $[Cu_2(1\text{-}TAN)_8(\mu\text{-}1\text{-}TAN)_2](ClO_4)_4$ is formed. The structure of the coordination sphere is displayed in Figure 5. For reason of clarity the non-coordinating perchlorate anions are not shown. The compound crystallized in the triclinic space group $P\bar{1}$ with one formula unit per unit cell. Both, the angles and the coordination bond lengths describe two highly distorted octahedra which are bridged by two 1-TAN ligands *via* the nitrogen atoms in 3- and 4-position of the tetrazole ring. The $N8^{i}$–Cu bond of these bridging ligands shows an especially increased bond length of 2.831 Å, clarifying the occupation of the z^2-axis together with a terminal tetrazole ligand (2.260 Å). The ligand's substituents take up positions in which they avoid steric interaction by stacking like saw teeth.

$[Cu(2\text{-}TAN)_2(\mu\text{-}2\text{-}TAN)_2](ClO_4)_2$ (Figure 6) demonstrates yet another coordination mode of the tetrazolylacetonitrile ligands. Since the bridging capabilities of the tetrazole ring are majorly influenced by the steric demand of the side-chain, the 3-position of the tetrazole ring is blocked in 2-TAN. This allows for the nitrile's coordination to the copper center in the elongated z^2-axis, while the tetrazole rings occupy the *xy*-plane. Ultimately, a two-dimensional coordination polymer is formed. As expected, the densities of the three copper perchlorates $[Cu(1\text{-}TAN)_6](ClO_4)_2$, $[Cu_2(1\text{-}TAN)_8(\mu\text{-}1\text{-}TAN)_2](ClO_4)_4$, and the polymeric ECC $[Cu(2\text{-}TAN)_2(\mu\text{-}2\text{-}TAN)_2](ClO_4)_2$ increase with increasing connectivity between the copper(II) centers from 1.654 (**5**), over 1.719 (**6**) to 1.777 g cm^{-3} (**11**) recalculated to room temperature.

Figure 7 shows the coordination structure of $[Ag(ClO_4)(\mu\text{-}1\text{-}TAN)]$ (**10**) in which each molecule of 1-TAN coordinates to three silver(I) centers. The polymeric structure is completed by coordination of the perchlorate anions. In combination, a 3D-polymeric network is formed. **10** crystallizes in the monoclinic space group *C*2/*c* with a high density of 2.539 g cm^{-3} at the measurement temperature of 123 K. The high density of the polymeric network, in combination with the heavy silver(I) cations and the ideal ratio of ligand to perchlorate, that, in theory, allows for the formation of gaseous N_2, CO, H_2O and HCl next to elemental silver as the only solid product, are a good prerequisite for a high-performing primary explosive.

In contrast, $[Ag(\mu\text{-}2\text{-}TAN)_2](ClO_4)$ (**12**) crystallizes in the monoclinic space group *P*2/*c* with a significantly lower density compared to **10**. The density of 2.159 g cm^{-3} at 123 K can again be explained by the polymeric network. Unlike 1-TAN, 2-TAN can only bridge between two silver(I) centers. This leads to the formation of a 1D-polymeric chains, which are intercalated by disordered perchlorate anions (Figure 8). This reduces the space filling of the structure compared to $[Ag(ClO_4)(\mu\text{-}1\text{-}TAN)]$. In

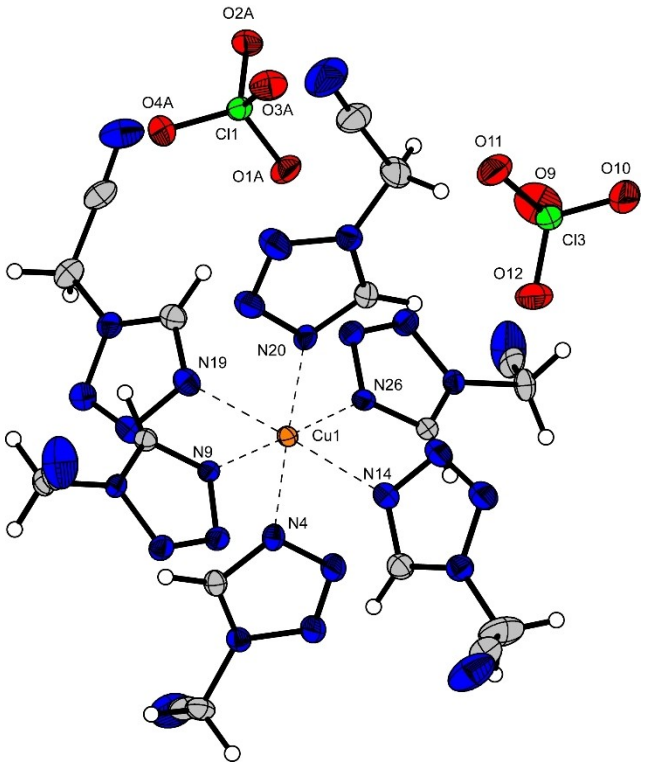

Figure 4. Coordination sphere of $[Cu(1\text{-}TAN)_6](ClO_4)_2$. Selected bond lengths [Å]: Cu1–N4 2.058(2), Cu1–N9 2.028(2), Cu1–N14 2.366(2), Cu1–N19 2.321(2), Cu1–N20 2.054(2), Cu1–N26 2.027(2); Selected bond angles [°]: N4–Cu1–N9 89.34(8), N4–Cu1–N14 87.89(8), N4–Cu1–N19 91.12(8), N4–Cu1–N20 177.70(8), N4–Cu1–N26 91.00(8), N9–Cu1–N14 91.24(8), N9–Cu1–N19 86.56(8), N9–Cu1–N20 91.35(8), N9–Cu1–N26 178.56(8), N14–Cu1–N19 177.59(8), N14–Cu1–N20 89.90(8), N14–Cu1–N26 90.18(8), N19–Cu1–N20 91.12(8), N19–Cu1–N26 92.04(8), N20–Cu1–N26 88.37(8).

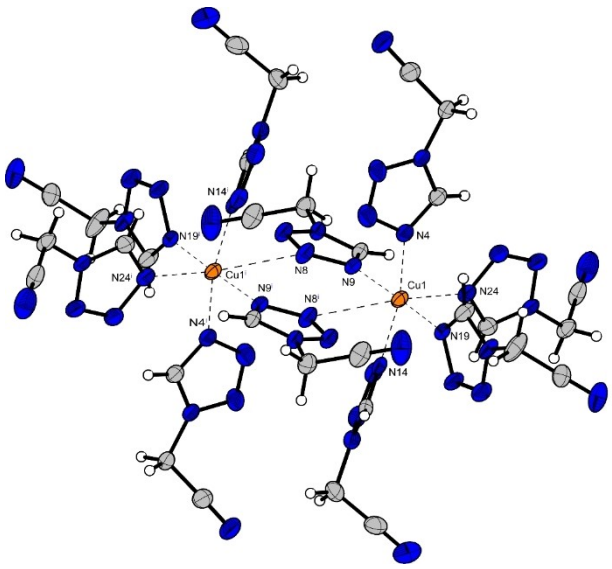

Figure 5. Coordination sphere of $[Cu_2(1\text{-}TAN)_8(\mu\text{-}1\text{-}TAN)_2](ClO_4)_4$. Selected bond lengths [Å]: Cu1–N4 2.015(3), Cu1–N9 2.022(3), Cu1–N14 2.011(3), Cu1–N19 2.034(3), Cu1–N24 2.260(3), Cu1–N8^{i} 2.831(3); Selected bond angles [°]: N4–Cu1–N9 87.75(12), N4–Cu1–N14 167.12(13), N4–Cu1–N19 90.01(12), N4–Cu1–N24 99.80(13), N4–Cu1–N8^{i} 89.33(12), N9–Cu1–N14 89.08(12), N9–Cu1–N19 175.06(13), N9–Cu1–N24 93.72(12); Symmetry codes: (i): 1−x, 1−y, 1−z.

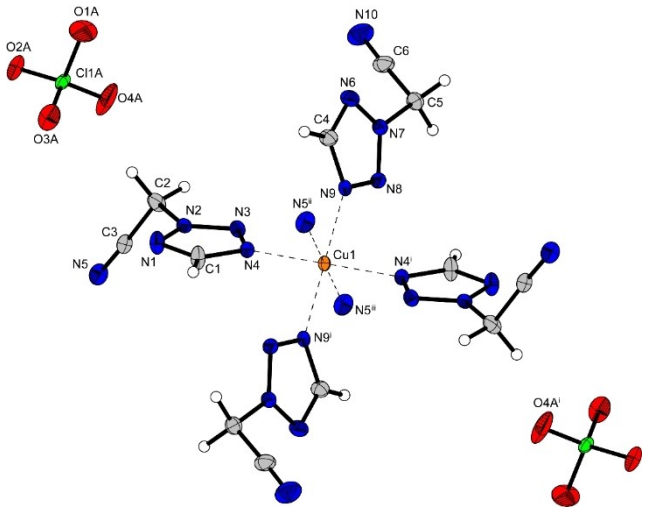

Figure 6. Coordination sphere of $[Cu(2\text{-}TAN)_2(\mu\text{-}2\text{-}TAN)_2](ClO_4)_2$. Selected bond lengths [Å]: Cu1–N4 1.9976(17), Cu1–N9 2.0341(17), Cu1–N5^{ii} 2.3442(19); Selected bond angles [°]: N4–Cu1–N9 89.11(7), N4–Cu1–N5^{ii} 89.49(7), N5^{ii}–Cu1–N9 88.01(7); Symmetry codes: (i): 2−x, 1−y, 1−z; (ii): 3/2−x, −1/2+y, 1/2−z; (iii): 1/2+x, 3/2−y, 1/2+z.

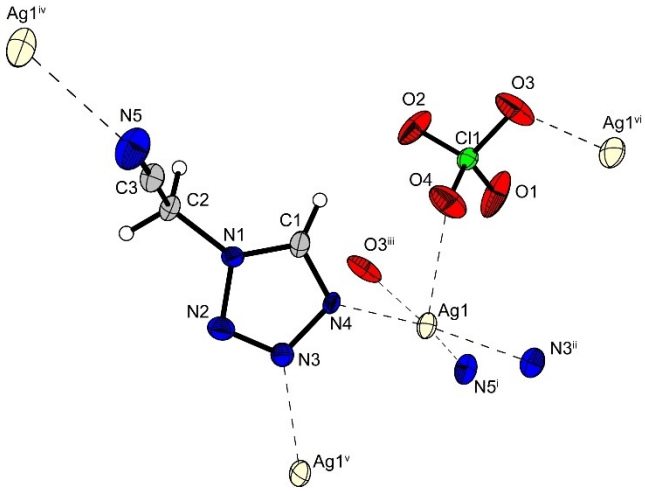

Figure 7. Coordination sphere of $[Ag(ClO_4)(\mu\text{-}1\text{-}TAN)]$. Selected bond lengths [Å]: Ag1–N4 2.244(4), Ag1–N5^{i} 2.356(5), Ag1–N3^{ii} 2.348(4); Selected bond angles [°]: N4–Ag1–N5 146.09(14), N4–Ag1–N3 121.50(15), N3–Ag1–N5 85.60(15); Symmetry codes: (i): 1/2+x, 1/2+y, z; (ii): 1/2−x, −1/2+y, 1/2−z; (iii): x, 1+y, z; (iv): −1/2+x, −1/2+y, z; (v): 1/2−x, 1/2+y, 1/2−z.

addition, the ratio of ligand to perchlorate and therefore fuel to oxidizer is increased compared to **10**.

In summary, the 1- and 2-TAN ligands show coordinative behavior as described in Figure 9. While 1-TAN can act as a bridging ligand at two positions of the tetrazole ring and the nitrile, 2-TAN only shows coordination at the 4-position of the ring, in addition to the nitrile. This behavior was observed in the cases of copper(II) and silver(I) perchlorates by low temperature X-ray diffraction. For compound **15** a similar behavior is estimated to lead to the composition $[Cu(TNR)(\mu\text{-}1\text{-}TAN)]$.

The structure of $[Cu(N_3)(1\text{-}TMT)]\cdot H_2O$ (**23**), as seen in Figure 10, was obtained by dissolving sodium azide and 1-TAN in water. On top, a mixture of water and ethanol (1:1) was

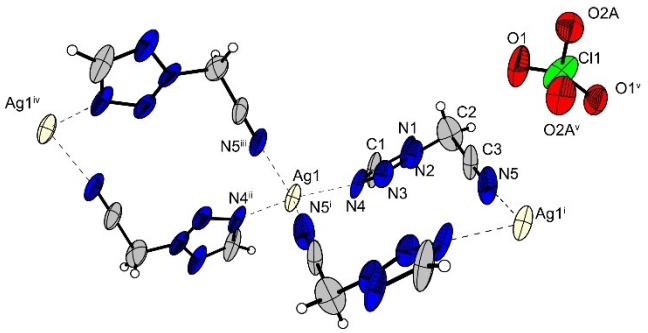

Figure 8. Coordination sphere of $[Ag(\mu\text{-}2\text{-}TAN)_2](ClO_4)$. Selected bond lengths [Å]: Ag1–N4 2.239(4), Ag1–N5 2.446(4); Selected bond angles [°]: N4–Ag1–N4^{ii} 145.17(19), N4–Ag1–N5^{i} 95.19(13), N4–Ag1–N5^{iii} 111.29(16); Symmetry codes: (i): 2−x, 1−y, 1−z; (ii): 2−x, y, 1/2−z; (iii): x, 1−y, −1/2+z; (iv): 2−x, 1−y, −z; (v): 1−x, y, 3/2−z.

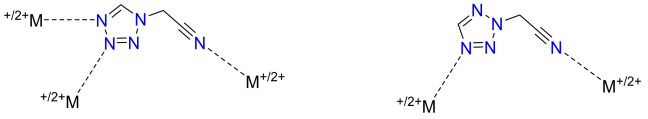

Figure 9. Schematic overview of the coordinative behaviour of 1- and 2-TAN.

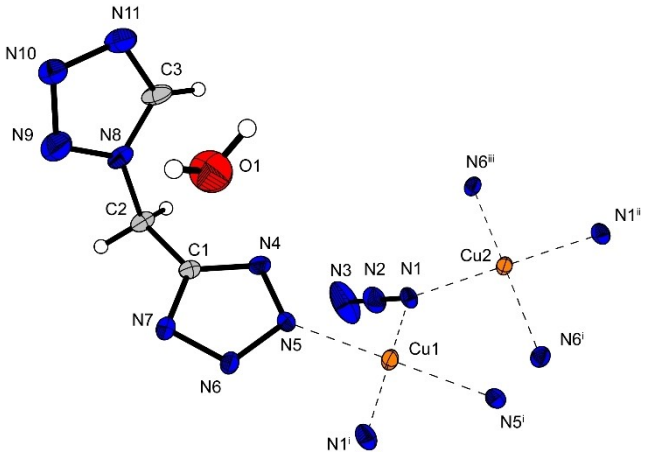

Figure 10. Crystal structure of $[Cu(N_3)(1\text{-}TMT)]\cdot H_2O$. Selected bond lengths [Å]: Cu1–N1 1.990(3), Cu1–N5 1.993(3), Cu2–N6^{iii} 1.997(3), Cu2–N1 1.992(3); Selected bond angles [°]: N1–Cu2–N6^{iii} 93.60(11), N1–Cu1–N5 93.54(11), Cu1–N1–Cu2 114.32(13); Symmetry codes: (i): 1−x, −y, 1−z; (ii): −x, −y, 1−z; (iii): −1+x, y, z.

poured, followed by an ethanolic solution of copper(II) nitrate trihydrate. Slow diffusion of the separate phases leads to formation of **23** as a green single crystal. The cyclization which formed the 1-TMT anion might have taken place by copper catalysis. Both, the tetrazolate and the azide anion bridge between two copper(II) centers each in coordination modes which have been previously described by the groups of Li and Sañudo.[26] Hereby, two dimensional porous networks are formed in which water was incorporated.

Energetic properties

The properties of the nitrogen-rich compounds **1**–**4** are listed in Table 1. The enthalpies of formation of the condensed phases were calculated using the atomization method of each room temperature CBS-4M enthalpy. Further details about the calculation are given in the Supporting Information. The enthalpies of formation of each compound were used for determination of the detonation parameters at the Chapman-Jouguet point by EXPLO5 (V7.01.01.).[25b] In addition, using CrystalExplorer, Hirshfeld calculations of compounds **1**, **3** and **4** were performed to get an insight into the interactions with neighboring molecules.[27] As expected, mainly stabilizing interactions were observed. The results are shown in the Supporting Information. To get an insight in the sensitivity of the ECCs, thermal analysis was conducted by DTA (OZM DTA 551-EX) or DSC (Mettler-Toledo DSC822e). Endothermic signals were further investigated by TGA (Perkin Elmer TGA4000) and for melting points with a Büchi B-540 device. A thermal stability of above 150 °C is often considered as a necessity for primary explosives.[28] This benchmark is reached for most of the compounds, except for $[Cu(1\text{-}TAN)_6](NO_3)_2$ (**7**), $[Ag(\mu\text{-}2\text{-}TAN)_2](ClO_4)$ (**12**), $[Cu(\mu\text{-}1\text{-}TAN)(TNR)]$ (**15**), and $[Cu(N_3)(2\text{-}TMT)]\cdot H_2O$ (**24**). The impact and friction sensitivities were obtained by applying the 1 of 6 method with BAM standard devices. Electrostatic discharge values were measured with the OZM XSpark10 device. These values clarify, that the ECCs should be handled with extreme caution, as most of them are categorized as very sensitive or sensitive to impact as well as

Table 1. Physiochemical properties of compounds **1**–**4**.

	1-TAN	2-TAN	1-HTMT	2-HTMT
Formula	$C_3H_3N_5$	$C_3H_3N_5$	$C_3H_4N_8$	$C_3H_4N_8$
M [g mol^{-1}]	109.09	109.09	152.12	152.12
IS [J][a]	>40	>40	10	15
FS [N][b]	>360	>360	360	360
ESD [J][c]	1.5	–	1.0	0.5
T_{endo}/T_{exo} [°C]	42/164	–/195	136/165	97/176
ρ [g cm^{-3}]	1.50[d]	1.30[e]	1.62[d]	1.61[d]
N [%] [f]	64.20	64.20	73.66	73.66
$\Delta_f H°$ [kJ mol^{-1}][g]	432.1	426.0	578.6	564.9
EXPLO5 V7.01.01				
$-\Delta_{Ex}U$ [kJ kg^{-1}][h]	3767	3844	3778	3691
$T_{det.}$ [K][i]	2703	2737	2715	2677
V_0 [L kg^{-1}][j]	646	661	707	708
P_{CJ} [kbar][k]	159	114	208	203
$V_{det.}$ [m s^{-1}][l]	6759	6202	7716	7636

[a] Impact sensitivity (BAM drophammer (1 of 6)). [b] Friction sensitivity (BAM friction tester (1 of 6)). [c] Electrostatic discharge devise (OZM XSpark10). [d] From X-ray diffraction analysis recalculated to 298 K. [e] Pycnometrically determined. [f] Nitrogen content. [g] Enthalpy of formation. [h] Energy of explosion. [i] Detonation temperature. [j] Volume of detonation products (assuming only gaseous products). [k] Detonation pressure at the Chapman - Jouguet point. [l] Detonation velocity.

Table 2. Thermal stability and sensitivities to mechanical and electrical stimuli of compounds **5**–**24**. Compounds **5a**, **13** and **18** are excluded for purity reasons.

Compound	No.	T_{endo}[a] [°C]	T_{exo}[b] [°C]	IS[c] [J]	FS[d] [N]	ESD[e] [mJ]	HP[f]	HN[g]
$[Cu(1\text{-}TAN)_6](ClO_4)_2$	**5**	–	173	<1	108	33	Def.	Def.
$[Cu_2(1\text{-}TAN)_8(\mu\text{-}1\text{-}TAN)_2](ClO_4)_4$	**6**	–	177	<1	60	160	Def.	Det.
$[Cu(1\text{-}TAN)_6](NO_3)_2$	**7**	75	117	>40	>360	106	Dec.	Dec.
$[Fe(1\text{-}TAN)_6](ClO_4)_2$	**8**	–	188	2	60	33	Def.	Def.
$[Zn(1\text{-}TAN)_6](ClO_4)_2$	**9**	–	180	10	240	1080	Dec.	Dec.
$[Ag(ClO_4)(\mu\text{-}1\text{-}TAN)]$	**10**	–	173	<1	1	5	Def.	Def.
$[Cu(2\text{-}TAN)_2(\mu\text{-}2\text{-}TAN)_2](ClO_4)_2$	**11**	–	190	<1	1.5	13	Def.	Det.
$[Ag(\mu\text{-}2\text{-}TAN)_2](ClO_4)$	**12**	–	67	<1	6	5	Def.	Det.
$[Cu(HTNR)_2(1\text{-}TAN)_2]$	**14**	–	205	3	240	63	Def.	Dec.
$[Cu(\mu\text{-}1\text{-}TAN)(TNR)]$	**15**	–	143	2	160	63	Dec.	Dec.
$[Cu(PA)_2(1\text{-}TAN)_2]$	**16**	–	170	2	>360	106	Comb.	Dec.
$[Cu(HTNO)_2(1\text{-}TAN)_2]$	**17**	–	181	2	360	63	Dec.	Dec.
$[Cu(HTNR)_2(2\text{-}TAN)_2]$	**19**	–	192	3	160	250	Comb.	Dec.
$[Cu(2\text{-}TAN)_2(TNR)]\cdot 0.5\ H_2O$	**20**	–	170	2	>360	250	Def.	Dec.
$[Cu(PA)_2(2\text{-}TAN)_2]$	**21**	–	194	3	>360	480	Comb.	Comb.
$[Cu(HTNO)_2(2\text{-}TAN)_2]$	**22**	–	174	2	288	480	Comb.	Dec.
$[Cu(N_3)(1\text{-}TMT)]\cdot H_2O$	**23**	–	208	<1	50	6	Det.	Det.
$[Cu(N_3)(2\text{-}TMT)]\cdot H_2O$	**24**	–	128	<1	7.5	13	Det.	Det.

[a] Onset temperature of endothermic event in the DTA or DSC (heating rate of 5 °C min^{-1}), indicating a melting point of the compound. [b] Onset of exothermic event in the DTA or DSC. [c] Impact sensitivity (BAM drophammer (1 of 6)). [d] Friction sensitivity (BAM friction tester (1 of 6)). [e] Electrostatic discharge devise (OZM XSpark10). [f] Hot plate test (det.: detonation, def.: deflagration, dec.: decomposition, comb.: combustion). [g] Hot needle test (det.: detonation, def.: deflagration, dec.: decomposition, comb.: combustion). [h] Endo-to-exo-transition.

sensitive to friction according to the "UN Recommendations on the Transport of Dangerous Goods".[29] An overview of the values is given in Table 2. By performing hot plate and hot needle tests, an insight into the behavior of rapid heating in open and confined environments is gained. While detonations and sharp deflagrations indicate potential use as a replacement of lead azide in detonator setups, which can be further tested by priming tests, combustion or decomposition of the material excludes the substance from potential use.

The capability of the promising substances to initiate PETN was tested in detonator setups. Therefore, 200 mg of PETN with a grain size below 100 μm was filled into a copper shell and pressed by lowering a weight of 8 kg onto. The shell was then placed on a copper witness plate. The substance of question (50 mg) was filled loosely on top, and a type A igniter was crimped to the top of the shell. Initiation was considered successful if a hole in the witness plate was observed. Incomplete initiation of PETN was observed in most tests, leading to deformation of the shell, which was then stuck on the witness plate. Only in the case of $[Ag(ClO_4)(\mu\text{-}1\text{-}TAN)]$ successful propagation of the detonation was feasible as seen in Figure 11. This is especially interesting because of the facile preparation. 1-TAN can be obtained without cost- and time-consuming column chromatography by tetrazole ring closure on the commercially available 2-aminoacetonitrile hydrochloride.[30] Since TGA revealed the loss of water of compound **23** at temperatures below 50 °C, it was dried at 80 °C until no OH stretch was visible in the IR. It's capability to initiate PETN was tested in this setup in its hydrated and dried form. In both cases the result was negative.

Figure 11. PETN initiation setup. Left: negative attempt with no damage to shell or plate, right: positive initiation by **10**.

Additionally, all colored ECCs were tested for laser initiation. Therefore, approximately 25 mg of substance were pressed into translucent polycarbonate primer caps with a force of 1.5 kN. The primer caps were then sealed by UV-curable adhesive and tested for their reaction to irradiation with a single pulsed laser. The InGaAs laser diode operates with a theoretical maximum power output of 45 W at a wavelength of 915 nm. The sample was placed in the focal distance of the optical lens and irradiated according to the parameters seen in Table 3. The irradiation of $[Cu_2(1\text{-}TAN)_8(\mu\text{-}1\text{-}TAN)_2](ClO_4)_4$ (**6**) and [Cu(2-

Table 3. Priming capability and laser ignitability results of the relevant ECCs.

Compound	No.	PETN initiation	Laser parameters[a]			
			6 A, 1 ms, 4 V	7 A, 1 ms, 4 V	7 A, 15 ms, 4 V	10 A, 30 ms, 4 V
$[Cu(1\text{-}TAN)_6](ClO_4)_2$	**5**	Neg.	–	–	Dec.	Dec.
$[Cu_2(1\text{-}TAN)_8(\mu\text{-}1\text{-}TAN)_2](ClO_4)_4$	**6**	Neg.	Det.	Det.	Det.	–
$[Cu(1\text{-}TAN)_6](NO_3)_2$	**7**	–	–	–	Dec.	Dec.
$[Fe(1\text{-}TAN)_6](ClO_4)_2$	**8**	–	–	–	Comb.	Def.
$[Ag(ClO_4)(\mu\text{-}1\text{-}TAN)]$	**10**	Pos.	–	–	–	–
$[Cu(2\text{-}TAN)_2(\mu\text{-}2\text{-}TAN)_2](ClO_4)_2$	**11**	Neg.	Det.	Det.	Det.	–
$[Ag(\mu\text{-}2\text{-}TAN)_2](ClO_4)$	**12**	Neg.	–	–	–	–
$[Cu(HTNR)_2(1\text{-}TAN)_2]$	**14**	–	–	–	–	Dec.
$[Cu(\mu\text{-}1\text{-}TAN)(TNR)]$	**15**	–	–	–	–	Dec.
$[Cu(PA)_2(1\text{-}TAN)_2]$	**16**	–	–	–	–	Dec.
$[Cu(HTNO)_2(1\text{-}TAN)_2]$	**17**	–	–	–	–	Dec.
$[Cu(HTNR)_2(2\text{-}TAN)_2]$	**19**	–	–	–	–	Dec.
$[Cu(2\text{-}TAN)_2(TNR)]\cdot 0.5\ H_2O$	**20**	–	–	–	–	Dec.
$[Cu(PA)_2(2\text{-}TAN)_2]$	**21**	–	–	–	–	Dec.
$[Cu(HTNO)_2(2\text{-}TAN)_2]$	**22**	–	–	–	–	Dec.
$[Cu(N_3)(1\text{-}TMT)]\cdot H_2O$	**23**	Neg.	Det.	Det.	–	–
$[Cu(N_3)(2\text{-}TMT)]\cdot H_2O$	**24**	Neg.	Det.	Det.	–	–

[a] Operating parameters: voltage U = 4 V, current I = 6–10 A, pulse length τ = 1–30 ms, theoretical maximal output power P_{max} = 45 W, wavelength λ = 915 nm (Det.: detonation, Def.: deflagration, Dec.: decomposition, Comb.: combustion, Neg.: negative).

$TAN)_2(\mu\text{-}2\text{-}TAN)_2](ClO_4)_2$ (**11**), with their improved ligand to perchlorate ratio due to bridging, showed violent detonations. Especially the comparison between $[Cu(1\text{-}TAN)_6](ClO_4)_2$ (**5**), which decomposes, and **6** is interesting since the minor stoichiometric change leads to such a major difference in performance. This discrepancy cannot be explained by differences of the thermal stabilities as both **6** and **11** show higher decomposition temperatures than **5**. Both, $[Cu(N_3)(1\text{-}TMT)]\cdot H_2O$ (**23**) and $[Cu(N_3)(2\text{-}TMT)]\cdot H_2O$ (**24**) were used in only 10 mg scale for the laser initiation to prevent damage to the setup by their strong detonation that was observed during hot plate and hot needle tests. The output, especially of **23**, qualifies it as a potent compound for laser-ignitable primer caps with moderate sensitivities and high thermal stability.

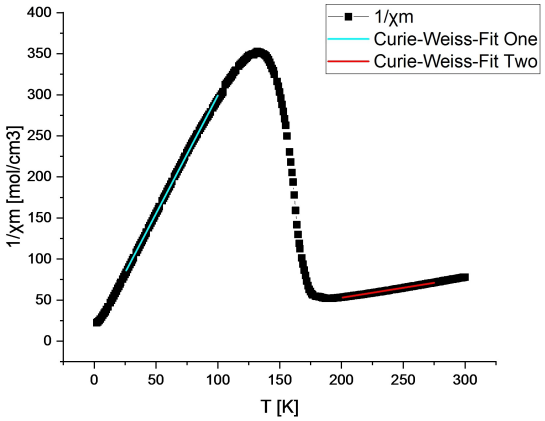

Figure 12. Inverted plot of the molar magnetic susceptibility of $[Fe(1\text{-}TAN)_6](ClO_4)_2$ at a field strength of $B = 3\ T$. The two Curie-Weiss-Fits (cyan for $T < 125\ K$ and red for $T > 170\ K$) indicate effective magnetic moments of $\mu_{eff} = 1.6676 \pm 0.00303\ \mu_B$ below 125 K and $\mu_{eff} = 5.74723 \pm 0.01407\ \mu_B$ above 170 K.

Magnetic properties

Since a thermochromic effect of $[Fe(1\text{-}TAN)_6](ClO_4)_2$ was observed during the low-temperature X-ray diffraction analysis, the magnetic properties of the coordination compound were further investigated. Magnetization measurements were performed with a Quantum Design Inc. physical property measurement system, which is equipped with a vibrating sample magnetometer. The sample was measured in a temperature range of 2–300 K at a field of ±30 kOe with the PPMS *MultiVu* software package.[31] Figure 12 shows the temperature-dependent spin-crossover behavior of the compound, which explains the change of color from colorless at room temperature to purple while cooling in the nitrogen stream. The difference between the effective momentum μ_{eff} and the theoretical value might be explained by the aging of the iron(II) perchlorate hexahydrate and subsequent oxidation to iron(III).[32] Similar observations have been reported for other thermally induced switches from the high spin $^5T_2$ to low spin $^1A_1$ population in octahedral iron(II) coordination compounds with different types of ligands.[33] The bond lengths, that can be observed for the Fe(II)–N coordination bond, show a clear reaction to the spin crossover by shortening from 2.1680(14) Å at 193 K to

1.9925(15) Å at 93 K. Such changes of close to 0.2 Å have been previously described for other examples in literature.[34]

Conclusions

The four nitrogen-rich ligands 1-TAN, 2-TAN, 1-HTMT and 2-HTMT were successfully synthesized and applied to energetic coordination compounds. A total of 21 ECCs was produced of which 18 were analyzed by X-ray diffraction analysis, supporting the structural variety of the coordination modes, which were expected from the ligands. Hereby, it was possible to alter the ratio of ligand to anion for the copper(II) perchlorates in a way that allowed laser initiation at low energies. The case of $[Ag(ClO_4)(\mu\text{-1-TAN})]$, which was used as a primary explosive to initiate a charge of PETN, supports the idea, that structural optimization of the ligand allows for an improvement of the ratio of fuel to oxidizer and therefore the performance of an energetic material. This is of special interest, since the ligand can be produced relatively cost efficient from commercially available chemicals. As a second, highly interesting ECC, $[Cu(N_3)(1\text{-TMT})]\cdot H_2O$ was characterized as an option for thermally and mechanically stable laser priming caps. Additionally, the magnetic properties of $[Fe(1\text{-TAN})_6](ClO_4)_2$ were studied, revealing a high-spin to low-spin transition below 170 K.

Supporting Information

The authors have cited additional references within the Supporting Information.[21–24,25b,27,29,35]

Acknowledgements

We gratefully acknowledge the financial support of this work by the Ludwig-Maximilians-Universität München. The authors also thank Dr. Peter Mayer for his contributions to the crystallographic data and Mr. Stefan Huber for sensitivity measurements. Open Access funding enabled and organized by Projekt DEAL.

Conflict of Interests

The authors declare no conflict of interest.

Data Availability Statement

The data that support the findings of this study are available from the corresponding author upon reasonable request.

Keywords: Energetic materials · Metal-organic frameworks · Coordination modes · Spin crossover · X-ray diffraction

[1] a) K. Soai, A. Ookawa, *J. Org. Chem.* **1986**, *51*, 4000–4005; b) C. M. Suter, E. W. Moffett, *J. Am. Chem. Soc.* **1934**, *56*, 487–487.
[2] V. Y. Kukushkin, A. J. L. Pombeiro, *Inorg. Chim. Acta* **2005**, *358*, 1–21.
[3] M. S. M. Pearson-Long, F. Boeda, P. Bertus, *Adv. Synth. Catal.* **2017**, *359*, 179–201.
[4] a) P. R. Sruthi, S. Anas, *J. Polym. Sci.* **2020**, *58*, 1039–1061; b) R. J. H. Gregory, *Chem. Rev.* **1999**, *99*, 3649–3682.
[5] a) B. N. Storhoff, H. C. Lewis Jr, *Coord. Chem. Rev.* **1977**, *23*, 1–29; b) S. F. Rach, F. E. Kühn, *Chem. Rev.* **2009**, *109*, 2061–2080.
[6] a) S. R. Buzilova, Y. V. Brekhov, A. V. Afonin, G. A. Gareev, L. I. Vereshchagin, *Zh. Obshch. Khim.* **1989**, *25*, 1524–1528; b) T. M. Klapötke, J. Stierstorfer, in *Green Energetic Materials*, **2014**, pp. 133–178.
[7] C. Kling, D. Leusser, T. Stey, D. Stalke, *Organometallics* **2011**, *30*, 2461–2463.
[8] a) L. Mahalakshmi, D. Stalke, in *Structure and Bonding*, Springer Berlin Heidelberg, **2002**, pp. 85–115; b) F. Baier, Z. Fei, H. Gornitzka, A. Murso, S. Neufeld, M. Pfeiffer, I. Rüdenauer, A. Steiner, T. Stey, D. Stalke, *J. Organomet. Chem.* **2002**, *661*, 111–127.
[9] a) C. Zhang, T.-W. Wang, Z.-J. Lu, Z.-X. Yi, B.-L. Kuang, S. Bu, Z.-M. Xie, Y. Li, K. Wang, J.-G. Zhang, *J. Phys. Chem. C* **2023**, *127*, 12923–12930; b) T.-W. Wang, Z.-J. Lu, Z.-X. Yi, Z.-M. Xie, L. Zhang, B.-L. Kuang, Y. Li, J.-G. Zhang, *Cryst. Growth Des.* **2023**, *23*, 5528–5534.
[10] a) N. Szimhardt, M. H. H. Wurzenberger, A. Beringer, L. J. Daumann, J. Stierstorfer, *J. Mater. Chem. A* **2017**, *5*, 23753–23765; b) N. Szimhardt, M. H. H. Wurzenberger, L. Zeisel, M. S. Gruhne, M. Lommel, J. Stierstorfer, *J. Mater. Chem. A* **2018**, *6*, 16257–16272; c) M. H. H. Wurzenberger, M. S. Gruhne, M. Lommel, N. Szimhardt, T. M. Klapötke, J. Stierstorfer, *Chem. Asian J.* **2019**, *14*, 2018–2028; d) M. H. H. Wurzenberger, S. M. J. Endraß, M. Lommel, T. M. Klapötke, J. Stierstorfer, *ACS Appl. Energ. Mater.* **2020**, *3*, 3798–3806; e) M. Rösch, M. S. Gruhne, M. Lommel, S. M. J. Endraß, J. Stierstorfer, *Inorg. Chem.* **2023**, *62*, 1488–1507; f) S. M. J. Endraß, T. M. Klapötke, J. T. Lechner, J. Stierstorfer, *FirePhysChem* **2023**, *3*, 330–338.
[11] a) H. Tourani, M. R. Naimi-Jamal, M. G. Dekamin, *ChemistrySelect* **2018**, *3*, 8332–8337; b) D. Kumar, G. H. Imler, D. A. Parrish, J. n M. Shreeve, *J. Mater. Chem. A* **2017**, *5*, 16767–16775; c) T. M. Klapötke, C. M. Sabaté, M. Rasp, *Dalton Trans.* **2009**, 1825–1834; d) T. Wu, R. Zhou, D. Li, *Inorg. Chem. Commun.* **2006**, *9*, 341–345.
[12] M. H. H. Wurzenberger, V. Braun, M. Lommel, T. M. Klapötke, J. Stierstorfer, *Inorg. Chem.* **2020**, *59*, 10938–10952.
[13] R. E. Trifonov, V. A. Ostrovskii, *Russ. J. Org. Chem.* **2006**, *42*, 1585–1605.
[14] A. L. Wani, A. Ara, J. A. Usmani, *Interdiscip. Toxicol.* **2015**, *8*, 55–64.
[15] a) DIRECTIVE 2011/65/EU OF THE EUROPEAN PARLIAMENT and OF THE COUNCIL of 8 June 2011 on the restriction of the use of certain hazardous substances in electrical and electronic equipment, European Union, **2011**; b) COMMISSION DELEGATED DIRECTIVE (EU) 2021/647 of 15 January 2021 amending, for the purposes of adapting to scientific and technical progress, Annex III to Directive 2011/65/EU of the European Parliament and of the Council as regards an exemption for the use of certain lead and hexavalent chromium compounds in electric and electronic initiators of explosives for civil (professional) use, European Union, **2021**.
[16] a) M. M. Puszynski, N. Mehta, G. Cheng, K. D. Oyler, D. Fischer, T. M. Klapötke, J. Stierstorfer, *J. Inorg. Chem.* **2016**, *1*, 003; b) M. H. H. Wurzenberger, M. Lommel, M. S. Gruhne, N. Szimhardt, J. Stierstorfer, *Angew. Chem. Int. Ed.* **2020**, *59*, 12367–12370; c) M. H. H. Wurzenberger, M. S. Gruhne, M. Lommel, N. Szimhardt, J. Stierstorfer, *Materials Advances* **2022**, *3*, 579–591; d) H. Li, Y. Wang, Z. Wei, X. Yang, L. Liang, L. Xia, M. Long, Z. Li, T. Zhang, *Chem. Eng. J.* **2022**, *430*, 132739.
[17] Z. P. Demko, K. B. Sharpless, *J. Org. Chem.* **2001**, *66*, 7945–7950.
[18] a) T. L. Desmarias, M. Costa, *Curr. Opin. Toxicol.* **2019**, *14*, 1–7; b) L. Leyssens, B. Vinck, C. Van Der Straeten, F. Wuyts, L. Maes, *Toxicology* **2017**, *387*, 43–56; c) K. K. Das, R. C. Reddy, I. B. Bagoji, S. Das, S. Bagali, L. Mullur, J. P. Khodnapur, M. S. Biradar, *J. Mol. Struct.* **2019**, *30*, 141–152.
[19] a) Y.-F. Yan, J.-G. Xu, F. Wen, Y. Zhang, H.-Y. Bian, B.-Y. Li, N.-N. Zhang, F.-K. Zheng, G.-C. Guo, *Inorg. Chem. Front.* **2022**, *9*, 5884–5892; b) Y.-F. Yan, Q.-Y. Wang, M. Cui, H.-Y. Bian, Y.-F. Han, J.-G. Xu, F.-K. Zheng, G.-C. Guo, *Chem. Eng. J.* **2023**, *472*, 144982.
[20] Deposition numbers 2320800 (for **1**), 2320810 (for **3**), 2320794 (for **4**), 2320807 (for **5**), 2320809 (for **5a**), 2320808 (for **6**), 2320797 (for **7**) 2320799 (for **8** at 93 K), 2320804 (for **8** at 193 K), 2320796 (for **9**), 2320814 (for **10**), 2320802 (for **11**), 2320812 (for **12**), 2320815 (for **13**), 2320801 (for **14**), 2320813 (for **16**), 2320803 (for **17**), 2320805 (for **18**), 2320811 (for **19**), 2320806 (for **20**), 2320816 (for **22**) and 2320795 (for **23**) contain the supplementary crystallographic data for this paper.

These data are provided free of charge by the joint Cambridge Crystallographic Data Centre and Fachinformationszentrum Karlsruhe Access Structures service.
[21] O. V. Dolomanov, L. J. Bourhis, R. J. Gildea, J. A. K. Howard, H. Puschmann, *J. Appl. Crystallogr.* **2009**, *42*, 339–341.
[22] G. M. Sheldrick, *Acta Crystallogr. Sect. A* **2015**, *71*, 3–8.
[23] a) *SHELXL-97*, University of Göttingen, G. M. Sheldrick, Germany, **1997**; b) G. M. Sheldrick, *Acta Crystallogr. Sect. A* **2008**, *64*, 112–122.
[24] *Diamond – Crystal and Molecular Structure Visualization*, Crystal Impact, H. Putz, K. Brandenburg, Bonn, Germany.
[25] a) M. Sućeska, *Propellants Explos. Pyrotech.* **1991**, *16*, 197–202; b) *EXPLO5* V7.01.01, M. Sućeska, Zagreb, **2023**.
[26] Y.-B. Xie, L. Gan, E. Carolina Sañudo, H. Zheng, J. Zhao, M. Zhao, B. Wang, J.-R. Li, *CrystEngComm* **2015**, *17*, 4136–4142.
[27] P. R. Spackman, M. J. Turner, J. J. McKinnon, S. K. Wolff, D. J. Grimwood, D. Jayatilaka, M. A. Spackman, *J. Appl. Crystallogr.* **2021**, *54*, 1006–1011.
[28] N. Mehta, K. Oyler, G. Cheng, A. Shah, J. Marin, K. Yee, *Z. Anorg. Allg. Chem.* **2014**, *640*, 1309–1313.
[29] Impact: insensitive >40 J, less sensitive ≥ 35 J, sensitive ≥ 4 J, very sensitive ≤ 3 J; Friction: insensitive >360 N, less sensitive $=360$ N, sensitive <360 N and >80 N, very sensitive ≤ 80 N, extremely sensitive ≤ 10 N, According to: Recommendations on the Transport of Dangerous Goods, Manual of Tests and Criteria, 4th. Edition, New York-Geneva, **1999**.
[30] P. N. Gaponik, V. P. Karavai, Y. V. Grigor'ev, *Chem. Heterocycl. Compd.* **1985**, *21*, 1255–1258.
[31] *MultiVu*, Version 1.5.11, Quantum Design Inc., San Diego, USA, **2013**.
[32] S. Mugiraneza, A. M. Hallas, *Commun. Phys.* **2022**, *5*, 95, DOI: 10.1038/s42005-022-00853-y.
[33] a) P. Gütlich, A. B. Gaspar, Y. Garcia, *Beilstein J. Org. Chem.* **2013**, *9*, 342–391; b) B. N. Figgis, J. Lewis, in *Progress in Inorganic Chemistry*, **1964**, pp. 37–239; c) V. Braun, M. H. H. Wurzenberger, V. Weippert, J. Stierstorfer, *New J. Chem.* **2021**, *45*, 11042–11050; d) D. Plaza-Lozano, A. Conde-Gallardo, J. Olguín, *Eur. J. Inorg. Chem.* **2021**, *2021*, 2846–2856.
[34] E. Collet, P. Guionneau, *C. R. Chim.* **2018**, *21*, 1133–1151.
[35] a) *CrysAlisPRO*, Version 171.33.41, Oxford Diffraction Ltd, **2009**; b) *PLATON*, Utrecht University, A. L. Spek, The Netherlands, **1999**; c) L. J. Farrugia, *J. Appl. Crystallogr.* **2012**, *45*, 849; d) *Empirical absorption correction using spherical harmonics*, *implemented in SCALE3 ABSPACK scaling algorithm*, Version 171.33.41, CrysAlisPro Oxford Diffraction Ltd., **2009**; e) *APEX3*, Bruker AXS Inc., Madison, Wisconsin, USA, ; f) *Gaussian 09 A.02*, Gaussian Inc, M. J. Frisch, G. W. Trucks, H. B. Schlegel, G. E. Scuseria, M. A. Robb, J. R. Cheeseman, G. Scalmani, V.Barone, B. Mennucci, G. A. Petersson, H. Nakatsuji, M. Caricato, X. Li, H. P. Hratchian, A. F. Izmaylov, J. Bloino, G. Zheng, J. L. Sonnenberg, M. Hada, M. Ehara, K. Toyota, R. Fukuda, J. Hasegawa, M. Ishida, T. Nakajima, Y. Honda, O. Kitao, H. Nakai, T. Vreven, J. A. Montgomery Jr., J. E. Peralta, F. Ogliaro, M. Bearpark, J. J. Heyd, E. Brothers, K. N. Kudin, V. N. Staroverov, R. Kobayashi, J. Normand, K. Raghavachari, J. C. B. A. Rendell, S. S. Iyengar, J. Tomasi, M. Cossi, N. Rega, J. M. Millam, M.Klene, J. E. Knox, J. B. Cross, V. Bakken, C. Adamo, J. Jaramillo, R. Gomperts, R. E. Stratmann, O. Yazyev, A. J. Austin, R. Cammi, C. Pomelli, J. W. Ochterski, R. L. Martin, K. Morokuma, V. G. Zakrzewski, G. A. Voth, P. Salvador, J. J. Dannenberg, S. Dapprich, A. D. Daniels, O. Farkas, J. B. Foresman, J. V. Ortiz, J. Cioslowski, D. J. Fox, Wallingford, CT, USA, **2009**; g) J. W. Ochterski, G. A. Petersson, J. A. M. Jr, *J. Chem. Phys.* **1996**, *104*, 2598–2619; h) J. A. Montgomery Jr, M. J. Frisch, J. W. Ochterski, G. A. Petersson, *J. Chem. Phys.* **2000**, *112*, 6532–6542; i) L. A. Curtiss, K. Raghavachari, P. C. Redfern, J. A. Pople, *J. Chem. Phys.* **1997**, *106*, 1063–1079; j) E. F. C. Byrd, B. M. Rice, *J. Phys. Chem. A* **2006**, *110*, 1005–1013; k) B. M. Rice, S. V. Pai, J. Hare, *Combust. Flame* **1999**, *118*, 445–458; l) http://webbook.nist.gov/chemistry/, accessed Mai 2022; m) M. S. Westwell, M. S. Searle, D. J. Wales, D. H. Williams, *J. Am. Chem. Soc.* **1995**, *117*, 5013–5015; n) F. Trouton, *Philos. Mag.* **1884**, *18*, 54–57; o) NATO standardization agreement (STANAG) on explosives, impact sensitivity tests, no. 4489, According to: 1st Edition, **1999**; p) WIWEB-Standardarbeitsanweisung 4-5.1.02, Ermittlung der Explosionsgefährlichkeit, hier der Schlagempfindlichkeit mit dem Fallhammer **2002**; q) NATO standardization agreement (STANAG) on explosive, friction sensitivity tests, no. 4487, According to: 1st. Edition, **2002**; r) WIWEB-Standardarbeitsanweisung 4-5.1.03, Ermittlung der Explosionsgefährlichkeit oder der Reibeempfindlichkeit mit dem Reibeapparat **2002**; s) https://www.ozm.cz/, accessed December 2021; t) *UN Model Regulation: Recommendations on the Transport of Dangerous Goods – Manual of Tests and Criteria*, *section 13.4.2.3.3*, **2015**.

Manuscript received: January 15, 2024
Revised manuscript received: January 30, 2024
Accepted manuscript online: March 4, 2024
Version of record online: ■■, ■■

RESEARCH ARTICLE

2-(1*H*-Tetrazol-1-yl)acetonitrile (1-TAN), 2-(2*H*-tetrazol-2-yl)acetonitrile (2-TAN), 5-((1*H*-tetrazol-1-yl)methyl)-1*H*-tetrazole (1-HTMT) and 5-((2*H*-tetrazol-2-yl)methyl)-1*H*-tetrazole (2-HTMT) were used as nitrogen-rich ligands for energetic coordination compounds (ECCs). The obtained energetic materials were analyzed concerning their physiochemical properties, providing viable data on the safety of handling. The properties in laser-ignitable primers and in lead-free detonator assemblies were evaluated.

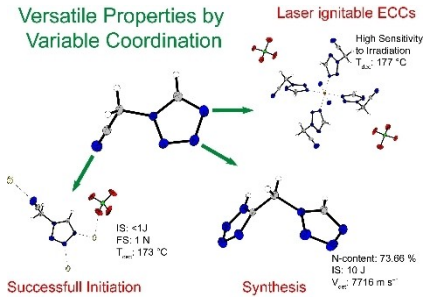

S. M. J. Endraß, Prof. Dr. T. M. Klapötke, M. Lommel, Dr. J. Stierstorfer, M. L. Weidemann, M. Werner*

1 – 11

1- and 2-Tetrazolylacetonitrile as Versatile Ligands for Laser Ignitable Energetic Coordination Compounds